amcs

FAULT DIAGNOSIS AND FAULT TOLERANT CONTROL USING SET–MEMBERSHIP APPROACHES: APPLICATION TO REAL CASE STUDIES

VICENÇ PUIG

Advanced Control Systems Group (SAC)
Technical University of Catalonia, Pau Gargallo, 5, 08028 Barcelona, Spain
e-mail: `vicenc.puig@upc.edu`

This paper reviews the use of *set-membership methods* in *fault diagnosis* (FD) and *fault tolerant control* (FTC). Set-membership methods use a deterministic unknown-but-bounded description of noise and parametric uncertainty (*interval models*). These methods aims at checking the consistency between observed and predicted behaviour by using simple sets to approximate the exact set of possible behaviour (in the *parameter* or the *state space*). When an inconsistency is detected between the measured and predicted behaviours obtained using a faultless system model, a fault can be indicated. Otherwise, nothing can be stated. The same principle can be used to identify interval models for fault detection and to develop methods for fault tolerance evaluation. Finally, some real applications will be used to illustrate the usefulness and performance of set-membership methods for FD and FTC.

Keywords: fault detection, fault-tolerant control, robustness, interval models, set-membership.

1. Introduction

Model-based fault detection of dynamic processes is based on the use of models i.e., (*analytical redundancy*) to check the consistency of the observed behaviour. However, when building a model of a dynamic process to monitor its behaviour, there is always some mismatch between the modelled and real behaviours since some effects are neglected, some non-linearities are linearised in order to simplify the model, some parameters have tolerance when compared between several units of the same component, some errors in parameters (or in the structure) of the model are introduced in the model calibration process, etc. These modelling errors introduce some uncertainty in the model. Usually, this uncertainty can be bounded and included in the fault detection model.

There are several ways of considering the uncertainty associated with the model depending if it is located in the parameters (*structured*) or in the model structure (*non-structured*). In the FD literature, a fault diagnosis algorithm able to handle uncertainty is called *robust*. The *robustness* of an FD algorithm is the degree of sensitivity to faults compared with the degree of sensitivity to uncertainty (Chen and Patton, 1999). Research on robust fault diagnosis methods has been very active in the FD community in the last few years. One of the most well-developed

families of approaches, called *active*, is based on generating residuals which are insensitive to uncertainty while at the same time sensitive to faults. This approach has been extensively developed by several researchers using different techniques: unknown input observers, robust parity equations, H_∞, etc. Chen and Patton (1999) present an excellent survey of this active approach.

On the other hand, there is a second family of approaches, called *passive*, which enhances the robustness of the fault detection system at the decision-making stage by propagating the uncertainty to the residuals and generating an *adaptive threshold*. Seminal papers suggesting this approach are the one by Horak (1988) in the time domain and that by Emami-Naeini *et al.* (1988) in the frequency domain. This passive approach has been developed lately by several researches but still is under development, see for example (Adrot and Flaus, 2008; Armengol *et al.*, 2008; Fagarasan *et al.*, 2004; Hamelin and Sauter, 2000; Ploix and Adrot, 2006; Puig *et al.*, 2006; 2008; Rambeaux, 2000; Sainz *et al.*, 2002). This approach has also been integrated with *qualitative reasoning* tools (coming from the AI community), see, e.g., the tools *CA~EN* (Travé-Massuyes *et al.*, 2001; Escobet *et al.*, 2001), *SQualTrack* (Armengol *et al.*, 2008) or *MOSES* (Rinner and Weiss, 2004). For a more detailed review, the reader is referred to the work of Armengol *et al.*

(2000).

This paper will review the passive approach when considering the nominal model plus uncertainty on every parameter bounded by intervals. This type of uncertainty modelling provides a type of models known as *interval models*. Noise will also be considered to be unknown but bounded and modelled in a deterministic framework. The use of interval models has received several names, depending on the field of application: in circuit analysis it is known as worst-case (or tolerance analysis), in automatic control as *set-membership* (also known in this field as the *error-bounded* approach) and in qualitative reasoning as semi-quantitative.

In the automatic control literature, the *set-membership* approach applied to parameter and state estimation was treated extensively by Milanese *et al.* (1996) while its application to control can be found in the works of Bhattacharyya *et al.* (1995) and Ackermann (2002). The worst-case analysis of circuits was treated by Kolev (1993) and in several research papers appearing in circuits journals and conferences. Finally, the semi-quantitative approach was investigated by Kuipers (1994) and in several papers appearing in artificial intelligence journals and conferences.

This paper also reviews the different approaches that can be used to identify interval models for fault detection. This research started with the seminal work of Ploix *et al.* (1999). New application fields for set-membership methods to areas close to FD as FTC are also presented. Finally, the paper presents several industrial applications where set-membership approaches have been successfully used.

The remainder of the paper is organized as follows. Section 2 introduces the use of interval models of dynamic systems for fault detection. In Section 3, fault detection using the interval approach is recalled, while Section 4 presents fault detection using the error-bounding approach. Section 5 reviews the methods for interval and error-bounding identification using real data. Section 6 presents the use of set-membership methods for fault tolerance evaluation of control laws. Section 7 presents several successful applications of set-membership methods for fault detection and fault-tolerant control. Finally, conclusions are summarised in Section 8.

2. Interval models of dynamic systems for fault detection

2.1. Interval models of dynamic systems.
The system to be monitored can be described by a MIMO linear uncertain dynamic model in discrete-time and a state-space form as follows:

$$\mathbf{x}(k+1) = \mathbf{A}(\boldsymbol{\theta})\mathbf{x}(k) + \mathbf{B}(\boldsymbol{\theta})\mathbf{u}(k) + \mathbf{w}(k),$$
$$\mathbf{y}(k) = \mathbf{C}(\boldsymbol{\theta})\mathbf{x}(k) + \mathbf{D}(\boldsymbol{\theta})\mathbf{u}(k) + \mathbf{v}(k), \quad (1)$$

where $\mathbf{y}(k) \in \mathbb{R}^{n_y}$, $\mathbf{u}(k) \in \mathbb{R}^{n_u}$, $\mathbf{x}(k) \in \mathbb{R}^{n_x}$ are the system output, input and state vectors, respectively, $\mathbf{w}(k) \in \mathbb{R}^{n_x}$ and $\mathbf{v}(k) \in \mathbb{R}^{n_y}$ are the disturbance and noise, respectively, both assumed unknown but bounded, i.e., $w_i \in \left[\underline{\delta}_i, \overline{\delta}_i\right]$ and $v_i \in [\underline{\sigma}_i, \overline{\sigma}_i]$; the state, input, output and direct transmission matrices are $\mathbf{A}(\boldsymbol{\theta}) \in \mathbb{R}^{n_x \times n_x}$, $\mathbf{B}(\boldsymbol{\theta}) \in \mathbb{R}^{n_x \times n_u}$, $\mathbf{C}(\boldsymbol{\theta}) \in \mathbb{R}^{n_y \times n_x}$ and $\mathbf{D}(\boldsymbol{\theta}) \in \mathbb{R}^{n_y \times n_u}$, respectively, $\boldsymbol{\theta} \in \mathbb{R}^{n_\theta}$ is the vector of uncertain parameters, where Θ is a bounded set (of the interval box type) such that and in particular for each component $\theta_i \in \left[\underline{\theta}_i, \overline{\theta}_i\right]$, $i = 1, \ldots, n_\theta$. This is why the resulting model is known as an interval model.

The set Θ contains all possible values of $\boldsymbol{\theta}$ when the system operates normally. Notice that when the parameters $\boldsymbol{\theta}$ are scheduled with the operating point using some known scheduling function and variable, then the system (1) is known as a *linear parameter varying* (LPV) system (Rugh and Shamma, 2000). Intervals for uncertain parameters can also be inferred from real data as will be discussed in Section 5.

The system in Eqn. (1) can, alternatively, be expressed in the input-output form using the shift operator q^{-1} and assuming zero initial conditions as follows:

$$\mathbf{y}(k) = \mathbf{M}(q^{-1}, \boldsymbol{\theta})\mathbf{u}(k), \quad (2)$$

where $\mathbf{M}(q^{-1}, \boldsymbol{\theta})$ is given by

$$\mathbf{M}(q^{-1}, \boldsymbol{\theta}) = \mathbf{C}(\boldsymbol{\theta})(q\mathbf{I} - \mathbf{A}(\boldsymbol{\theta}))^{-1}\mathbf{B}(\boldsymbol{\theta}) + \mathbf{D}(\boldsymbol{\theta}).$$

2.2. Interval models for fault detection.
The principle of model-based fault detection is to test whether the system measurements are consistent with the behaviour described by a model of the faultless system. Consistent means that the measured system behaviour agrees with the behaviour estimated using the model. If the measurements are inconsistent with this model, the existence of a fault is proved. The residual vector, known also as an *analytical redundant relation* (ARR), defined as the difference between measured $\mathbf{y}(k)$ and predicted system outputs $\hat{\mathbf{y}}(k)$,

$$\mathbf{r}(k) = \mathbf{y}(k) - \hat{\mathbf{y}}(k), \quad (3)$$

is usually used to check the consistency.

Ideally, the residuals should only be affected by faults. However, the presence of disturbances, noise and modelling errors causes the residuals to become nonzero and thus interferes with the detection of faults. Therefore, the fault detection procedure must be robust against these undesired effects (Chen and Patton, 1999). In the case of modelling a dynamic system using an interval model, the predicted output is described by a set that can be bounded at any iteration by an interval

$$\hat{y}_i(k) \in [\underline{\hat{y}_i}(k), \overline{\hat{y}_i}(k)] \quad (4)$$

in a non-faulty case. Such an interval is computed independently for each output (neglecting couplings between outputs) as follows:

$$\underline{\hat{y}_i}(k) = \min_{\boldsymbol{\theta}\in\Theta}(\hat{y}_i(k,\boldsymbol{\theta})) \ \text{ and } \ \overline{\hat{y}_i}(k) = \max_{\boldsymbol{\theta}\in\Theta}(\hat{y}_i(k,\boldsymbol{\theta})). \tag{5}$$

Such an interval can be computed using the algorithm based on numerical optimization presented by Puig *et al.* (2003). Then, the fault detection test is based on propagating parameter uncertainty to the residual, and checking if

$$\mathbf{y}(k) \in \left[\underline{\hat{\mathbf{y}}}(k) - \sigma, \overline{\hat{\mathbf{y}}}(k) + \sigma \right], \tag{6}$$

where σ is the noise bound. Equivalently, the previous test can be formulated in terms of the residual checking whether or not

$$0 \in [\underline{\mathbf{r}}(k), \overline{\mathbf{r}}(k)] = \mathbf{y}(k) - \left[\underline{\hat{\mathbf{y}}}(k) - \sigma, \overline{\hat{\mathbf{y}}}(k) + \sigma \right] \tag{7}$$

holds. In case it does not hold, a fault can be indicated. This test is named a *direct test*.

Alternatively, an *inverse test* consists in checking if there exists some parameter value in the parameter uncertainty set Θ such that the model (2) is consistent with the system measurements. More formally, we check the condition

$$\exists \boldsymbol{\theta} \in \Theta \mid \hat{\mathbf{y}}(k,\boldsymbol{\theta}) \in [\mathbf{y}(k) - \sigma, \mathbf{y}(k) + \sigma]. \tag{8}$$

In case this condition is not satisfied, a discrepancy between measurements and the model is detected and a fault should be indicated. This test can be implemented with parameter estimation algorithms used in the error-bounding approach (Milanese *et al.*, 1996), as will be discussed later in this paper. The direct test is related to the use of the parity equation or observer methods, while the inverse test is related to parameter estimation methods. According to Isermann (2006), parity equations and observer approaches are more suitable for additive faults, while the parameter estimation approach is better suited for multiplicative (parametric) faults.

3. Fault detection using the interval approach

3.1. Fault detection using interval observers.
The system described by Eqn. (1) can be monitored using a linear observer with the *Luenberger structure*. The resulting *interval observer* can be written as

$$\begin{aligned} \hat{\mathbf{x}}(k+1,\boldsymbol{\theta}) &= \mathbf{A}(\boldsymbol{\theta})\hat{\mathbf{x}}(k) + \mathbf{B}(\boldsymbol{\theta})\mathbf{u}(k) + \mathbf{w}(k) \\ &\quad + \mathbf{L}(\mathbf{y}(k) - \hat{\mathbf{y}}(k)), \\ \hat{\mathbf{y}}(k,\boldsymbol{\theta}) &= \mathbf{C}(\boldsymbol{\theta})\hat{\mathbf{x}}(k) + \mathbf{v}(k), \end{aligned} \tag{9}$$

where $\hat{\mathbf{x}}(k,\boldsymbol{\theta})$ is the estimated state-space vector and $\hat{\mathbf{y}}(k,\boldsymbol{\theta})$ is the estimated output vector for a given value

of $\boldsymbol{\theta} \in \Theta$ taking into account process and sensor noise bounds. The observer gain matrix $\mathbf{L} \in \mathbb{R}^{nx \times ny}$ is designed to stabilize the matrix $\mathbf{A}_o(\boldsymbol{\theta})$ and to guarantee the desired performance regarding fault detection for all $\boldsymbol{\theta} \in \Theta$ (Chilali and Gahinet, 1996). Alternatively, the observer given by Eqn. (9) can be expressed in the input-output form using the q-transform and considering zero initial conditions as follows:

$$\hat{\mathbf{y}}(k) = \mathbf{G}(q^{-1},\boldsymbol{\theta})\mathbf{u}(k) + \mathbf{H}(q^{-1},\boldsymbol{\theta})\mathbf{y}(k), \tag{10}$$

where

$$\begin{aligned} \mathbf{G}(q^{-1},\boldsymbol{\theta}) &= \mathbf{C}(\boldsymbol{\theta})\left(q\mathbf{I} - \mathbf{A}_o(\boldsymbol{\theta})\right)^{-1}\mathbf{B}(\boldsymbol{\theta}), \\ \mathbf{H}(q^{-1},\boldsymbol{\theta}) &= \mathbf{C}(\boldsymbol{\theta})\left(q\mathbf{I} - \mathbf{A}_o(\boldsymbol{\theta})\right)^{-1}\mathbf{L}, \\ \mathbf{A}_o(\boldsymbol{\theta}) &= \mathbf{A}_o(\boldsymbol{\theta}) - \mathbf{L}\mathbf{C}(\boldsymbol{\theta}). \end{aligned}$$

Interval observation requires solving the optimization problems introduced in Eqn. (5) using Eqn. (10). In order to preserve *uncertain parameter time-invariance* and to avoid the *wrapping effect* [1] (Puig *et al.*, 2003), the observer output prediction in Eqn. (5) is substituted by

$$\begin{aligned} \hat{\mathbf{y}}(k) &= \mathbf{C}(\boldsymbol{\theta})\,\mathbf{A}_0(\boldsymbol{\theta})^k\,\mathbf{x}_0 \\ &\quad + \mathbf{C}(\boldsymbol{\theta})\sum_{j=0}^{k-1}\mathbf{A}_0(\boldsymbol{\theta})^{(k-1-j)}\,\mathbf{B}(\boldsymbol{\theta})\,\mathbf{u}(j). \end{aligned} \tag{11}$$

When proceeding in this way, the optimization problems in Eqn. (11) will not be convex because of the nonlinearity with respect to parameters. Therefore, the existence of a unique optimum is not guaranteed. In order to guarantee that the global optimum is reached, a global optimization algorithm must be used. In particular, a branch and bound interval arithmetic global optimization based on *Hansen's algorithm* (Hansen, 1992) can be used. An additional computational problem appears when using Eqn. (11), since the degree of the polynomial in the objective function increases with time. This implies that the amount of computation needed also increases with time, being impossible to operate over a large time period. This problem can be solved if the interval system (1) is asymptotically stable (Puig *et al.*, 2003). In this case, the predicted system output at time k depends, approximately, only on the inputs that occurred in a *time sliding window* with a length ℓ (whose value is of the order of the settling time) and the state at the beginning of such a window. Then, Eqn. (11) can be approximated by limiting the computation to a finite time horizon as proposed by Puig *et al.* (2003).

---

[1]The problem of wrapping is related to the use of a crude approximation of the set of states associated with the interval simulation. If, at each iteration, the true solution set is wrapped into its interval hull, since the overestimation of the wrapped set is proportional to its radius, a spurious growth of the enclosures may result if the composition of wrapping and mapping is iterated.

If uncertain parameters are considered *time-varying*, an iterative algorithm can be used that obtains the set of uncertain states at time k, $\mathbb{X}_k$ from the set $\mathbb{X}_{k+1}$ using the algorithm presented in Fig. 1 (Guerra *et al.*, 2008).
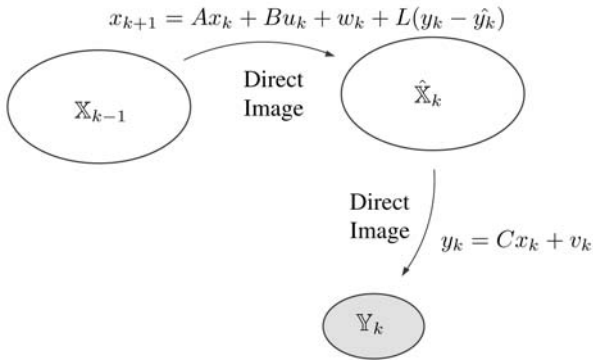

Fig. 1. Interval observer.

To implement such an algorithm, the set of uncertain states should be approximated since the exact set of estimated states would be difficult to compute. Several geometrical shapes have been proposed in the literature ranging from parallelotopes (Chisci *et al.*, 1996) or ellipsoids (Maksarov and Norton, 1996) to zonotopes (Alamo *et al.*, 2005). A zonotope $\mathbb{X}$ of order m can be viewed as the Minkowski sum of m segments:

$$\mathbb{X} = \mathbf{p} \oplus \mathbf{H}B^m = \{\mathbf{p} + \mathbf{Hz} : \mathbf{z} \in B^m\}, \qquad (12)$$

where the segments are defined by the columns of matrix $\mathbf{H}$ and B^m is a unitary box composed of m unitary intervals. The order m is a measure for the geometrical complexity of the zonotopes (see Fig. 2 for a zonotope of order 14).
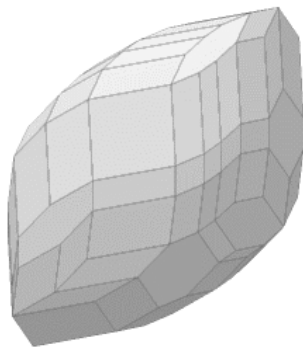

Fig. 2. Zonotope.

Zonotope arithmetic possesses a set of operations (such as sum, affine transformation, intersection) that can be very efficiently implemented since they only involve operations with matrices (Alamo *et al.*, 2005).

3.2. Interval ARMA parity equations.

If the observer gain in Eqn. (9) is assumed to be equal to zero ($\mathbf{L} = 0$), the observer becomes an *interval simulator*, since the output prediction is based only on the inputs and previous output predictions, and Eqn. (10) becomes

$$\hat{\mathbf{y}}(k) = \mathbf{M}(q^{-1}, \boldsymbol{\theta})\mathbf{u}(k),$$

while the residual is given by

$$\mathbf{r}(k) = \mathbf{y}(k) - \hat{\mathbf{y}}(k) = \mathbf{y}(k) - \mathbf{M}(q^{-1}, \boldsymbol{\theta})\mathbf{u}(k). \quad (13)$$

According to Gertler (1998), Eqn. (13) corresponds to an *ARMA primary parity equation* or *residual*. This is an *open-loop approach*. Interval simulation requires solving optimization problems following the same strategy as in the case of the interval observer but using the system matrices (1). In order to reduce the computing complexity, as in the observer case, a time window could also be used. In this case, this approach is known as the ℓ-order ARMA parity equation (Tornil *et al.*, 2003).

3.3. Interval MA parity equations.

On the other hand, if the observer gain in Eqn. (8) is designed such that the poles are at the origin (*deadbeat observer*), the observer becomes an *interval predictor*, since the output prediction is based only on measured inputs and outputs and follows the real system output after the minimum number of samples. The prediction equation (10) is a moving average (MA) and follows a *closed-loop approach*. Thus, the corresponding residuals are called *MA primary parity equations* or *residuals* (Gertler, 1998). The optimization problems (5) that must be solved now are linear with respect to the parameters and, therefore, convex. This means that there exist very efficient algorithms to solve them (as the *simplex algorithm*). Because of the linearity, the existence of a unique optimum is guaranteed to be located at one of the vertices of the parameter uncertainty intervals. Interval prediction is not affected by the problem of wrapping because the predicted output is based on the previous output measurements instead of the interval of the previous predicted outputs (Puig *et al.*, 2008). Thus, interval prediction considers uncertain parameters as time varying. But, time invariance in uncertain parameters being to be preserved, an ℓ-order MA parity equation should be used (Tornil *et al.*, 2003). Finally, Ploix and Adrot (2006) proposed a method to obtain the interval parity equations directly from the state-space using the *Chow-Wilsky scheme*.

3.4. Comparison.

In the work of Puig *et al.* (2008), the behaviour of the different interval fault detection approaches considered so far is studied and compared using the FD benchmark proposed in the DAMADICS project. Table 1 summarises the results of this comparison. This

table can be used as a guideline to decide in which applications an approach is more suitable than others. Prediction and simulation approaches have antagonistic properties: prediction, because of its deadbeat observer behaviour, does not suffer from the wrapping effect and low computational complexity, has low sensitivity to unmodeled dynamics but can suffer from the sensor following fault effect and has high sensitivity to sensor noise. On the other hand, the simulation approach exhibits opposite properties, presenting good performance when detecting sensor faults in noisy systems. Finally, the observer approach is in the middle, with the advantage that, since it has one more degree of freedom (the observer gain), it can be designed trying to minimize the bad effects and maximize the good effects of the other two approaches.

Table 1. Interval-based fault detection approaches features.

Issue		Simulator	Observer	Predictor
Wrapping effect		Yes	Yes	No
Computational complexity		High	High	Low
Unmodeled dynamics sensitivity		High	Medium	Low
Initial conditions sensitivity		High	Medium	Low
Fault sensitivity	actuator	Dynamic	Dynamic	Constant
	sensor	Constant	Pulse	Deadbeat
Noise sensitivity	process	LP filter	LP filter	Gain
	sensor	Gain	HP Filter	HP filter

4. Fault detection using the error-bounding approach

Alternatively to the interval approach presented in the previous section, the error-bounding approach relies on checking whether the measured sequence of system inputs and outputs available at every time instant k could have been generated by the model (2) and parameter values in the parameter uncertainty set Θ (Ocampo *et al.*, 2006). This approach is related to the inverse test described in Section 2.

4.1. Fault detection test in the parameter space. The inverse test involves checking if there exists a parameter in the parameter uncertainty set Θ_k such that the model (2) is consistent with the systems measurements. This test can be easily implemented using the error-bounding parameter estimation procedure described in Section 5 since it can operate in the recursive form as follows:

$$\Theta_{k+1} = \Theta_k \cap \mathbb{F}_k, \qquad (14)$$

where

$$\mathbb{F}_k$$
$$= \left\{ \boldsymbol{\theta} \in \mathbb{R}^{n_\theta} | \mathbf{y}(k) - \sigma \leq \mathbf{M}(q^{-1}, \boldsymbol{\theta})\mathbf{u}(k) \leq \mathbf{y}(k) + \sigma \right\}$$

is the strip of parameters consistent with the current measurements. In fault detection using the inverse test, the

model is assumed invalidated and a fault is indicated if $\Theta_{k+1} = \emptyset$ (Ingimundarson *et al.*, 2008). Once the fault has been indicated, the feasible parameter set Θ_k should be reset to a set that contains all possible values even in a faulty situation. Then, the faulty feasible parameter set can be identified (fault isolation) and the fault size can be estimated by comparing the feasible parameter set before and after fault detection using, for example, the distance between centres of these sets (fault estimation).

Although outer approximation is most often used in fault detection since it contains all the consistent models, inner approximation, which contains only consistent parameters, can complement the use of outer approximation in order to improve the fault detection behaviour.

4.2. Fault detection test in the state space. An error-bounded state estimator assumes *a priori* bounds on noise and uncertain parameters and constructs sets of estimated states that are consistent with the *a priori* bounds and current measurements. Several researchers (Chisci *et al.*, 1996; Maksarov and Norton, 1996; Shamma, 1997; Calafiore, 2001; Kieffer *et al.*, 2002) have addressed this issue. Consider the system given by Eqn. (1), an initial compact set $\mathbb{X}_o$ and a sequence of measured inputs and outputs, the uncertain state set at time k using the error-bounding approach can be computed using the algorithm presented in Fig. 3. A fault is detected when $\mathbb{X}_k^e = \mathbb{X}_k^p \cap \mathbb{X}_k^y = \emptyset$ (Planchon and Lunze, 2006; Guerra *et al.*, 2007).
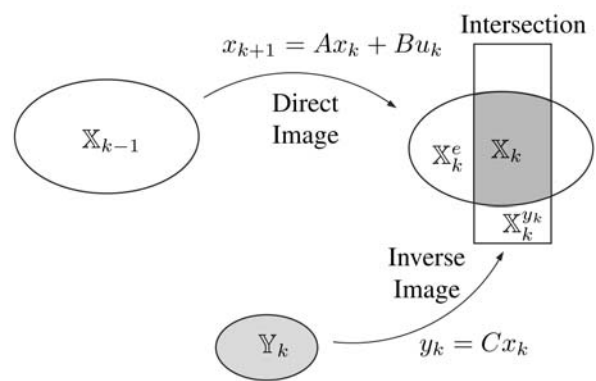

Fig. 3. Error-bounding state estimation.

5. Identification for robust fault detection

5.1. Model parametrisation. One of the key points in model based fault detection is how models are calibrated to fit real data taken from the monitored system in non-faulty situations. Identification should deliver a calibrated nominal model plus its modelling error in the

form of interval parameters, which will provide an interval of confidence for predicted behaviour, i.e., the interval model, as already discussed in the introduction of this paper. To this aim, several authors (Campi and Calafiore, 2009; Calafiore *et al.*, 2002; Ploix *et al.*, 1999) suggested an adaptation of classical system identification methods to provide the nominal model plus the uncertainty intervals for parameters that guarantee that all recorded data from the system in non-faulty scenarios will be included in the interval model. These algorithms are based on using classical identification methods (for example, least-squares) to provide the nominal estimate for system parameters. Then the intervals of uncertainty for parameters are adjusted until all the measured data are covered by the model prediction interval.

These algorithms proceed considering that the interval model (1) to be identified can be expressed in the regressor form as follows:

$$y(k) = \boldsymbol{\varphi}^T(k)\boldsymbol{\theta} + v(k) = \hat{y}(k) + v(k), \qquad (15)$$

where $\varphi(k)$ is the regressor vector of dimension n_θ which can contain any function of inputs $u(k)$ and outputs $y(k)$; $v(k)$ is additive noise bounded by a constant $|v(k)| \leq \sigma$; $\theta \in \Theta_k$ is the parameter vector of dimension n_θ and Θ_k is the set that bounds parameter values. This set can again be approximated by ellipsoids, parallelotopes or zonotopes (Milanese *et al.*, 1996). If this set is described by a zonotope centered in the nominal model, it can be parameterised as follows (Bravo *et al.*, 2006):

$$\Theta_k = \boldsymbol{\theta}^0 \oplus \mathbf{H}B^n = \left\{ \boldsymbol{\theta}^0 + \mathbf{H}\mathbf{z} : \mathbf{z} \in B^n \right\}. \qquad (16)$$

Notice that a particular case corresponds to the case where the parameter set Θ_k is an interval box:

$$[\theta_i] = [\theta_i^{\min}, \theta_i^{\max}] = [\theta_i^0 - \lambda_i, \theta_i^0 + \lambda_i] \qquad (17)$$

with $i = 1, \ldots, n_\theta$. This set can be viewed as a zonotope with $\mathbf{H}$ equal to an $n_\theta \times n_\theta$ diagonal matrix:

$$\mathbf{H} = \text{diag}(\lambda_1, \lambda_2, \ldots, \lambda_{n_\theta}). \qquad (18)$$

Given a sequence of M regressor vector values $\varphi(k)$ in a fault free scenario and a model parameterised as in Eqn. (15), the aim is to estimate model parameters and their uncertainty (model set) following either an *interval* or *error-bounding parameter estimation* approach.

5.2. Interval parameter estimation. In this case, the set of uncertain parameters Θ_k should be obtained in such a way that all measured data in a fault free scenario will be covered by the predicted output interval produced by using the model (15) and the uncertainty parameter set, that is,

$$\overline{\hat{y}}(k) \geq y(k) - \sigma \ \text{ and } \ \underline{\hat{y}}(k) \leq y(k) + \sigma, \ \ \forall k = 1, \ldots, M, \qquad (19)$$

where

$$\overline{\hat{y}}(k) = \max \left(\boldsymbol{\varphi}^T(k)\boldsymbol{\theta} \right) \qquad \text{with } \boldsymbol{\theta} \in \Theta_k, \qquad (20a)$$

$$\underline{\hat{y}}(k) = \min \left(\boldsymbol{\varphi}^T(k)\boldsymbol{\theta} \right) \qquad \text{with } \boldsymbol{\theta} \in \Theta_k. \qquad (20b)$$

This type of model identification was first suggested by Ploix *et al.* (1999) in the context of fault detection using a direct test and an interval LTI model in prediction.

Assuming that the parameter set Θ_k can be described as the zonotope (16) and proceeding as Ploix *et al.* (1999), the maximum and minimum interval prediction bounds provided by the model (15) are given by

$$\overline{\hat{y}}(k) = \hat{y}^0(k) + \left\| \boldsymbol{\varphi}^T(k)\mathbf{H} \right\|_1, \qquad (21a)$$

$$\underline{\hat{y}}(k) = \hat{y}^0(k) - \left\| \boldsymbol{\varphi}^T(k)\mathbf{H} \right\|_1, \qquad (21b)$$

where $\hat{y}^0(k)$ is the model output prediction with nominal parameters, i.e., $\hat{y}^0(k) = \boldsymbol{\varphi}^T(k)\theta^0$ where $\boldsymbol{\theta}^0 = (\theta_1^0, \ldots, \theta_{n_\theta}^0)$.

Notice that in the particular case of interval parameters

$$\left\| \boldsymbol{\varphi}^T(k)\mathbf{H} \right\|_1 = \sum_{i=1}^{n} \lambda_i \left| \boldsymbol{\varphi}_i(k) \right| \qquad (22)$$

replacing Eqns. (21a) and (21b) in the inclusion conditions (19), the optimal zonotope that fulfills the *interval prediction condition* can be computed using *Algorithm* 1. In this algorithm, the cost function f in Algorithm 1 is usually the interval prediction thickness that can be calculated as

$$\sum_{k=1}^{N} \left(\overline{\hat{y}}(k) - \underline{\hat{y}}(k) \right) = 2 \sum_{k=1}^{N} \left\| \boldsymbol{\varphi}^T(k)\mathbf{H} \right\|_1. \qquad (23)$$

Algorithm 1 Interval parameter estimation (general case).

$$\min_{\mathbf{H}} \ f(\Theta_{\mathbf{k}}(\mathbf{H}))$$

subject to

$$\left\| \boldsymbol{\varphi}^T(k)\mathbf{H} \right\|_1 \geq \left| y(k) - \hat{y}^0(k) \right| - \sigma, \quad \forall k = 1, \ldots, M$$

In order to reduce the complexity of Algorithm 1, the zonotope that bounds Θ_k can be parameterised such that $\mathbf{H} = \lambda \mathbf{H}_0$, corresponding with a zonotope with a predefined shape (determined by $\mathbf{H}_0$) and a scalar λ. Then, in this case, the interval prediction thickness (23) is given by

$$\sum_{k=1}^{N} \left(\overline{\hat{y}}(k) - \underline{\hat{y}}(k) \right) = 2 \left| \lambda \right| \sum_{k=1}^{N} \left\| \boldsymbol{\varphi}^T(k)\mathbf{H}_0 \right\|_1 = f(|\lambda|), \qquad (24)$$

and restrictions of Algorithm 1 can be expressed as follows:

$$\lambda \left\| \boldsymbol{\varphi}^T(k)\mathbf{H}_0 \right\|_1 \geq \left| y(k) - \hat{y}^0(k) \right| - \sigma, \qquad (25)$$

leading to

$$\lambda \geq \frac{\left|y(k) - \hat{y}^0(k)\right| - \sigma}{\left\|\boldsymbol{\varphi}^T(k)\mathbf{H}_0\right\|_1} \tag{26}$$

such that Algorithm 1 can be rewritten as Algorithm 2. The optimal solution provided by such algorithm is

$$\lambda = \sup_{k \in \{1,\ldots,M\}} \left(\frac{\left|y(k) - \hat{y}^0(k)\right| - \sigma}{\left\|\boldsymbol{\varphi}^T(k)\mathbf{H}_0\right\|_1} \right). \tag{27}$$

Algorithm 2 Interval parameter estimation (particular case).

$$\min_{\lambda} \ 2\left|\lambda\right| \sum_{k=1}^{N} \left\|\boldsymbol{\varphi}^{\mathrm{T}}(k)\mathbf{H}_0\right\|_1$$

subject to

$$\lambda \geq \frac{\left|y(k) - \hat{y}^0(k)\right| - \sigma}{\left\|\boldsymbol{\varphi}^T(k)\mathbf{H}_0\right\|_1}, \quad \forall k = 1, \ldots, M$$

5.3. Error-bounding parameter estimation. On the other hand, the set of uncertain parameters Θ_k using an error-bounded parameter estimation approach is obtained in such a way that the predicted behaviour is consistent with all the measured data in a fault-free scenario. In this case, the obtained model satisfies the assumption that the predicted behaviour is always inside the interval of possible measurements, that is,

$$\hat{y}(k) - \sigma \leq y(k) \leq \hat{y}(k) + \sigma, \quad \forall k = 1, \ldots, M, \tag{28}$$

where

$$\hat{y}(k) = \boldsymbol{\varphi}^T(k)\boldsymbol{\theta}$$

and $\boldsymbol{\theta} \in \Theta_k$.

Algorithms for identifying such a kind of model are also known as *bounded-error parameter estimation* algorithms. In the work of Milanese *et al.* (1996), there is a survey of such methods.

Using this approach, the parameter set Θ_k that contains all models consistent with data, known as the *feasible parameter set* (FPS), is defined as follows:

$$\mathbb{FPS} = \left\{ \boldsymbol{\theta} \in \Theta_k \mid y(k) - \sigma \leq \boldsymbol{\varphi}^T(k)\boldsymbol{\theta} \leq y(k) + \sigma, \right. \\ \left. k = 1, \ldots, M \right\}. \tag{29}$$

In general, the exact description of the $\mathbb{FPS}$ is not simple. For this reason, existing algorithms usually approximate the $\mathbb{FPS}$ using inner/outer simpler shapes such as boxes, ellipsoids or zonotopes (Milanese *et al.*, 1996). The approximation set is called an approximated feasible parameter set (AFPS). In this paper, algorithms that provide an inner/outer AFPS employing zonotopes when using the model parameterised as in (15) are presented.

5.3.1. Outer approximations. Outer approximation algorithms find the parameter set Θ_k of a minimum volume such that $\mathbb{FPS} \subseteq \Theta_k$. This kind of algorithm usually implies an excessive computational cost, and recursive forms have been proposed, such as the one described by Bravo *et al.* (2006). This recursive approach is based in computing iteratively the AFPS using zonotopes and related operations as follows:

$$\mathbb{AFPS}_{k+1} = \mathbb{AFPS}_k \cap \mathbb{F}_k \tag{30}$$

where

$$\mathbb{F}_k = \left\{ \boldsymbol{\theta} \in \mathbb{R}^{n_\theta} \mid y(k) - \sigma \leq \boldsymbol{\varphi}^T(k)\boldsymbol{\theta} \leq y(k) + \sigma \right\}.$$

5.3.2. Inner approximations. Inner approximation algorithms find the parameter set Θ_k of a maximum volume such that $\Theta_k \subseteq \mathbb{FPS}$.

A bounded-error inner approximation using zonotopes parameterised as in Eqn. (16) for models expressed as in (15) can be obtained in a similar way as proposed in Algorithm 2. The inner approximation algorithm comes from fact the FPS conditions (29) can be bounded by

$$y(k) - \sigma \leq \underline{\hat{y}}(k) \leq \boldsymbol{\varphi}^T(k)\boldsymbol{\theta} \leq \overline{\hat{y}}(k) \leq y(k) + \sigma,$$

where $\underline{\hat{y}}(k)$ and $\overline{\hat{y}}(k)$ are defined as in (20a)–(20b), respectively, and, if Θ_k is a zonotope, calculated as in (21a)–(21b). Then, the maximum inner zonotope, centered at $\boldsymbol{\theta}^0$, can be computed using Algorithm 3, where the cost function f in the error-bounded approach is usually the volume of the zonotope defined by (16). This volume only depends on matrix $\mathbf{H}$ and on B^n with a volume equal to 2^n. In the particular case, $\mathbf{H}$ is a square matrix ($n_\theta = n$), the volume is given by $\mathrm{vol}(\Theta_k) = 2^n \left|\det(\mathbf{H})\right|$. See the research by Montgomery (1989) for more details.

Algorithm 3 Inner bounded-error zonotope (general case).

$$\max_{\mathbf{H}} \ f(\Theta_{\mathbf{k}}(\mathbf{H}))$$

subject to

$$\left\|\boldsymbol{\varphi}^T(k)\mathbf{H}\right\|_1 \leq \sigma - \left|y(k) - \hat{y}^0(k)\right|, \quad \forall k = 1, \ldots, M$$

As in Algorithm 1, to reduce the computational complexity, the particular case when $\mathbf{H} = \lambda\mathbf{H}_0$ will be considered. Then, if H_0 is a square matrix, $\mathrm{vol}(\Theta_k) = \left|2\lambda\right|^n \left|\det(\mathbf{H}_0)\right|$ and restrictions of Algorithm 3 can be expressed as

$$\left\|\boldsymbol{\varphi}^T(k)\mathbf{H}_0\right\|_1 \leq \sigma - \left|y(k) - \hat{y}^0(k)\right|, \tag{31}$$

leading to

$$\lambda \leq \frac{\sigma - \left|y(k) - \hat{y}^0(k)\right|}{\left\|\boldsymbol{\varphi}^T(k)\mathbf{H}_0\right\|_1} \tag{32}$$

such that it can be rewritten as Algorithm 4. The optimal solution provided by such an algorithm is

$$\lambda = \inf_{k\in\{1,\dots,M\}} \left(\frac{\sigma - |y(k) - \hat{y}^0(k)|}{\|\varphi^T(k)\mathbf{H}_0\|_1} \right). \qquad (33)$$

Algorithm 4 Inner bounded-error zonotope (particular case).

$$\max_{\lambda} \ \text{vol}(\Theta_k) = f(|\lambda|)$$

subject to

$$\lambda \leq \frac{\sigma - |y(k) - \hat{y}^0(k)|}{\|\varphi^T(k)\mathbf{H}_0\|_1}, \quad \forall k = 1,\dots,M$$

---

6. Fault tolerance evaluation using set-membership approaches

6.1. Motivation. The objective of this section is to assess the tolerance of a certain actuator fault configuration considering a linear predictive/optimal control law with constraints showing the potential of set-membership methods for FTC. This issue has been already treated in the literature for the case of the LQR problem but without constraints (Staroswiecki, 2003), thanks to the existence of an analytical solution. However, constraints (on states and control signals) are always present in real industrial control problems and could be easily handled using _model predictive control_ (MPC). In general, an analytical solution for these kinds of control laws does not exist, which makes it difficult to reproduce the fault tolerance evaluation analysis proposed by Staroswiecki (2003). The method proposed in this section is not of analytical but of computational nature. It follows the idea proposed by Lydoire and Poignet (2005), in which the calculation of the control law for a predictive/optimal controller with constraints can be divided in two steps: first, the calculation of a solutions set that satisfies the constraints (_feasible solution set_), and then, optimal solution determination.

Faults in actuators will cause changes in the set of feasible solutions since constraints on control signals vary. This could make the set of admissible solutions for the control objective empty. Therefore, the admissibility of the control law facing actuator faults can be determined knowing the feasible solutions set. This section provides a method to compute this set and then evaluate the admissibility of the control law.

To find the feasible solutions set for the problem of MPC, a constraint satisfaction problem could be formulated (Ocampo _et al._, 2006). However, this problem is computationally demanding and should be solved approximately in an iterative way in time, bounding it by its inter-

val hull. Moreover, when proceeding in this way, an interval simulation problem is implicitly solved exhibiting typical difficulties associated with it (such as the wrapping effect, among others) (Puig _et al._, 2003), already described in Section 3. In order to avoid such problems, the set of possible states should be approximated using more complex domains than intervals. In this section, a zonotope-based method to evaluate the admissibility of fault actuator configurations is proposed and discussed.

6.2. Admissibility of the control law. The solution to a control problem consists in finding a control law in a given set of control laws $\mathbb{U}$ such that the controlled system achieves the _control objectives_ $\mathbb{O}$ while its behaviour satisfies a set of _constraints_ $\mathbb{C}$. The solution of the problem is completely defined by the triple $\langle \mathbb{U}, \mathbb{O}, \mathbb{C} \rangle$. In the case of a linear constrained predictive control law, it can be formulated as follows:

$$\mathbb{O} : \min_{\tilde{\mathbf{u}}} \ J(\tilde{\mathbf{x}}, \tilde{\mathbf{u}}),$$

subject to

$$\mathbb{C} : \begin{cases} \mathbf{x}_{k+1} = \mathbf{A}\mathbf{x}_k + \mathbf{B}\mathbf{u}_k, \\ \mathbf{u}_k \in \mathbb{U} \quad k = 1,\dots,N-1, \\ \mathbf{x}_k \in \mathbb{X} \quad k = 0,\dots,N, \end{cases}$$

where

$$\mathbb{U} = \left\{ \mathbf{u}_k \in \mathbb{R}^m | \ \mathbf{u}_{\min} \leq \mathbf{u}_k \leq \mathbf{u}_{\min} \right\},$$
$$\mathbb{X} = \left\{ \mathbf{x}_k \in \mathbb{R}^n | \ \mathbf{x}_{\min} \leq \mathbf{x}_k \leq \mathbf{x}_{\min} \right\}$$

and

$$\tilde{\mathbf{u}}_k = (\mathbf{u}_j)_0^{k-1} = (\mathbf{u}_0, \mathbf{u}_1, \dots, \mathbf{u}_{k-1}),$$
$$\tilde{\mathbf{x}}_k = (\mathbf{x}_j)_0^{k-1} = (\mathbf{x}_0, \mathbf{x}_1, \dots, \mathbf{x}_k).$$

The _feasible solution set_ is given by

$$\Omega = \left\{ \tilde{\mathbf{x}}, \tilde{\mathbf{u}} | \ (\mathbf{x}_{k+1} = \mathbf{A}\mathbf{x}_k + \mathbf{B}\mathbf{u}_k)_0^{N-1} \right\} \qquad (36)$$

and gives the input and state sets compatible with system constraints which originate the set of predictive states.

On the other hand, the _feasible control objectives set_ is given by

$$\mathcal{J}_\Omega = \left\{ J(\tilde{\mathbf{x}}, \tilde{\mathbf{u}}) | \ (\tilde{\mathbf{x}}, \tilde{\mathbf{u}}) \in \Omega \right\} \qquad (37)$$

and corresponds to the set of all values of $J(\tilde{\mathbf{x}}, \tilde{\mathbf{u}})$ obtained from feasible solutions in the set (36)

Finally, the _admissible solution set_ is given by

$$\mathbb{A} = \left\{ (\tilde{\mathbf{x}}, \tilde{\mathbf{u}}) \in \Omega_f | \ J(\tilde{\mathbf{x}}, \tilde{\mathbf{u}}) \in \mathcal{J}_A \right\}, \qquad (38)$$

where Ω_f corresponds to the feasible solution set of an actuator fault configuration and $\mathcal{J}_A$ is defined as the admissible control objective set according to controller specifications in a faulty situation. These specifications are given by the end user as part of the controller specifications.

The admissibility evaluation using a set computation approach starts obtaining the feasible solution set Ω introduced in (36) given a set of initial states $\mathbb{X}_o$, the system dynamics and the system operating constraints over N using Algorithm 5, which is represented graphically by Fig. 4.

Algorithm 5 Computation of the feasible solution set Ω.

1: $\mathbb{X}_0 \Leftarrow \mathbb{X}$
2: $\Omega_0 \Leftarrow \mathbb{X}_0 \times \mathbb{U}$
3: **for** $k = 1$ to N **do**
4:     $\mathbb{U}_{k-1} \Leftarrow \mathbb{U}$
5:     Compute $\mathbb{X}_k^p$ from $\mathbb{X}_{k-1}$ and $\mathbb{U}_{k-1}$ taking into account that

$$\mathbb{X}_k^p = \{x_k = Ax_{k-1} + Bu_{k-1} \,|\, x_{k-1} \in \mathbb{X}_{k-1},$$
$$u_{k-1} \in \mathbb{U}\}$$

6:     Compute $\mathbb{X}_k^c = \mathbb{X} \cap \mathbb{X}_k^p$
7:     Compute $\mathbb{U}_{k-1}^c$ from $\mathbb{X}_k^c$ and $\mathbb{X}_{k-1}^c$ taking into account that

$$\mathbb{U}_{k-1}^c = \{u_{k-1} \in \mathbb{U} \,|\, x_k = Ax_{k-1} + Bu_{k-1}$$
$$x_k \in \mathbb{X}_k^c, x_{k-1} \in \mathbb{X}_{k-1}^c\}$$

8:     $\Omega_k = \mathbb{X}_k^c \times \mathbb{U}_{k-1}^c$
9:     $\mathbb{X}_k \Leftarrow \mathbb{X}_k^c$
10: **end for**
11: $\Omega = \bigcup\limits_{k=0}^{N} \Omega_k$

While the feasible solution set Ω is being computed, the feasible control objectives set $\mathcal{J}_\Omega$ at time k can be obtained using Algorithm 6, which is represented by Fig. 5. A given fault actuator configuration is admissible if

$$\mathcal{J}_A \cap \mathcal{J}_\Omega \neq \emptyset.$$

Otherwise, it is not admissible.

Algorithm 6 Admissibility evaluation of a given actuator fault configuration (AFC) and some admissible control objective set $\mathcal{J}_A$.

1: $\mathbb{X}_k \Leftarrow \mathcal{X}_0$
2: $\Omega_0 \Leftarrow \mathcal{X}_0$
3: **for** $k = 1$ to N **do**
4:     Compute Ω_k using *Algorithm* 5
5:     Compute $\mathcal{J}_{\Omega_k}$ defined in Eq. (38)
6: **end for**
7: $\mathcal{J}_\Omega = \bigcup\limits_{k=0}^{N} \mathcal{J}_{\Omega_k}$
8: **if** $\mathcal{J}_A \cap \mathcal{J}_\Omega = \emptyset$ **then**
9:     AFC is *not admissible*
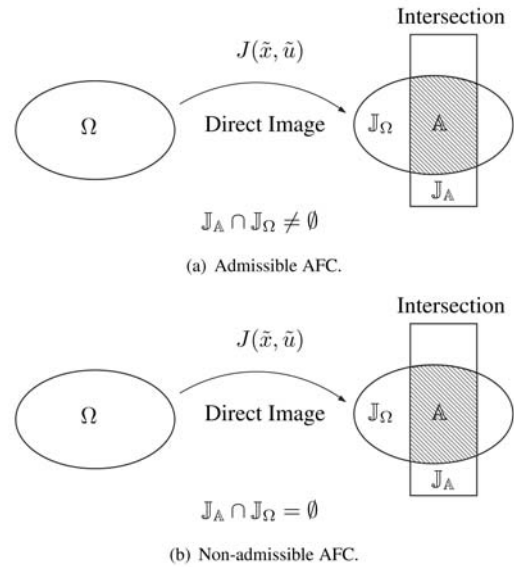10: **else**
11:     AFC is *admissible*
12: **end if**

(a) Admissible AFC.

(b) Non-admissible AFC.

Fig. 5. Admissibility evaluation: admissible AFC (a), non-admissible AFC (b).

Fig. 4. Feasible solution set computation.

More details on how Algorithms 5 and 6 can be implemented using zonotopes can be found in the work of Guerra *et al.* (2007).

7. Real applications

The FD/FTC set-membership methods described in this paper were used in some real applications, in which the Advanced Control Systems (SAC)[2] research group at Universitat Politècnica de Catalunya (UPC)[3] was deeply involved.

7.1. FD Application: DAMADICS case study.
DAMADICS was a Research Trained Network funded by the European Commission under the 5th Framework programme. It started in 2000 and ended in 2003. The objectives were providing the training and mobility of researchers working on the synthesis and development of methods and on-line diagnostic tools for applications in power, food processing and chemical industries. Within this network, a benchmark for fault diagnosis was developed based on an industrial smart actuator used in the evaporation station of a sugar factory in Poland (Bartyś *et al.*, 2006). The smart actuator consists of a control valve, a pneumatic servomotor and a smart positioner (see Fig. 6). In this paper, this benchmark will be used for testing and comparing the fault detection and identification methods presented in Sections 3 and 5. In particular, the focus will be on the pneumatic servomotor and the electro-pneumatic transducer components of the smart actuator (see Fig. 7).

Fig. 6. DAMADICS smart actuator.
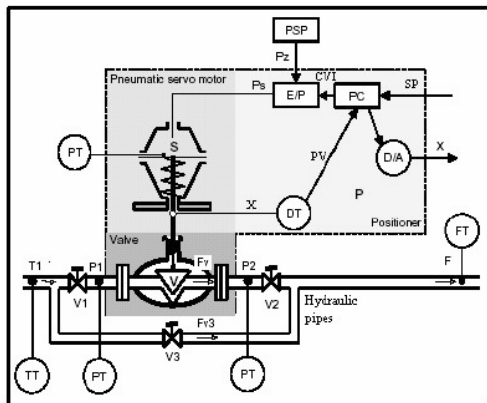
Fig. 7. DAMADICS smart actuator block diagram.

7.1.1. Interval model of the system. The pneumatic servomotor has non-linear second-order dynamics (Bartyś

and de las Heras, 2003) described by

$$m\frac{\mathrm{d}^2 X}{\mathrm{d}t^2} = -k_v \frac{\mathrm{d}X}{\mathrm{d}t} - k_x (k + X) + A_e P_s + mg, \quad (39)$$

where X is the servomotor rod displacement (neglecting hysteresis), P_s is the pressure in the servomotor chamber, A_e is the diaphragm area, m is the mass rod, k_x is the spring and diaphragm constant, k is a constant (0.00925) and k_v is the valve constant.

On the other hand, the electro-pneumatic transducer has non-linear first-order dynamics described by

$$\frac{\mathrm{d}P_s}{\mathrm{d}t} = (P_s + P_a) \left(\frac{1}{m_a} \frac{\mathrm{d}m_a}{\mathrm{d}t} - \frac{A_e}{V} \frac{\mathrm{d}X}{\mathrm{d}t} \right), \quad (40)$$

where A_e is the diaphragm area, CVP is the command pressure, P_a is the athmospheric pressure, P_s is the pressure in the servomotor's chamber, P_z is the positioner supply pressure, k_1 is a units conversion factor (2.5×10^{-6}), V is the chamber volume, R is the constant for ideal gases, T is the ambient temperature, $m_a = (P_s + P_a) V/RT$ is the air mass and $\mathrm{d}m_a/\mathrm{d}t$ is the air mass flow is given by

$$\frac{\mathrm{d}m_a}{\mathrm{d}t} = \begin{cases} k_1 CVP \sqrt{P_z - P_s} & \text{if} \quad CVP > 0, \\ k_1 CVP \sqrt{P_s} & \text{if} \quad CVP \leq 0. \end{cases} \quad (41)$$

Assuming that the volume V is constant and considering the case when $CVP > 0$, the discrete-time transfer function (in terms of the q-operator) that relates $X(k)$ with $CVP(k)$ can be obtained by replacing P_s in (39) by a linearised version of Eqn. (40):

$$X(k) = \frac{b_{x_2} q^{-2} + b_{x_3} q^{-3}}{1 + a_{x_1} q^{-1} + a_{x_2} q^{-2} + a_{x_3} q^{-3}} CVP(k). \quad (42)$$

Using this model for the servomotor and a scenario free of faults, an interval model for simulation, prediction and observation that will produce an interval for the predicted behaviour including all non-modelled effects, noise and modelling errors is derived using interval identification algorithms presented in Section 5. In the observer approach, the observer gain was pre-designed using the nominal parameters of the simulation approach such that it provides dynamics four times faster than the servomotor ($\mathbf{L} = [-0.1286 \quad -0.0087 \; 0.0717]$). It should be noticed that in Table 2 some parameters are not considered uncertain since after the interval identification process the obtained uncertainty is negligible.

7.2. Application to several fault scenarios.

7.2.1. Fault f_{10} ("*diaphragm perforation*"). In this scenario, a fault in the pneumatic servomotor is introduced. The fault is a servomotor diaphragm perforation caused by the fatigue of the diaphragm material. In the

Table 2. Interval model parameter estimation.

Parameter	Simulator	Predictor	Observer
a_{x_1}	0.0501	[0.0027, 0.0207]	[0.0485, 0.0517]
a_{x_2}	-0.0032	[0.0002, 0.0022]	-0.0032
a_{x_3}	[−0.8595, −0.8495]	[−1.5616, −1.5716]	-0.8545
b_{x_2}	[−0.6681, −0.6581]	[0.3570, 0.3590]	-0.6631
b_{x_3}	[0.5384, 0.5484]	[0.2111, 0.2311]	[0.5353, 0.5595]

DAMADICS benchmark, this fault is named as f_{10}. It the present experiments, the fault scenario that will be used corresponds to the abrupt big size (Bartys *et al.*, 2006). The fault appears at time instant $t = 2100$ s.

In Fig. 8, results of the interval simulation approach are presented. It can be observed that the real measurement goes out of the simulation envelope immediately and the fault indicator is activated permanently after fault appearance. This is one the main properties of the simulation approach since the output prediction only uses the input but not the output.

In Fig. 9, results of the interval prediction approach are presented. In this case, it can be observed that the measurement goes out of the prediction envelope. But, after some time instants, it comes back inside the envelope because of the use of output measurements to produce the output prediction. This is the *fault following effect* that is a feature of the prediction approach. The fault indicator is only activated when the measurement is outside the envelope, but when the measurement comes back inside the envelope, it is deactivated. Since this approach is very sensitive to noise, even when the measurement is inside the envelope, it can go out for a few seconds. Recall that the prediction approach is based on the previous measurements corrupted by the noise.

Finally, in Fig. 10, results of the interval observation are presented. In this case, the situation can be viewed as intermediate between the two previous approaches. The measurement goes out of the observation envelope when the fault appears. But because of partial measurement correction it comes back inside the envelope after 300 s of the initial fault detection time. Clearly, fault detection persistency is bigger than in the case of the prediction approach. Since this approach only corrects the prediction partially with measurements, the effect of noise is less important than in the case of the prediction approach, being the number of fault false indications due to the noise effect.

7.2.2. Fault f_1 (*"valve clogging"*). In this case, a fault in the control valve is introduced. The fault is *valve clogging*. It consists in blocking servomotor rod displacement by an external event of mechanical nature. In the DAMADICS benchmark, this fault is named as f_1. It the present experiments the fault scenario that will be used corresponds to the abrupt big size (Bartys *et al.*, 2006). The fault appears at time instant $t = 2100$ s. Results pre-
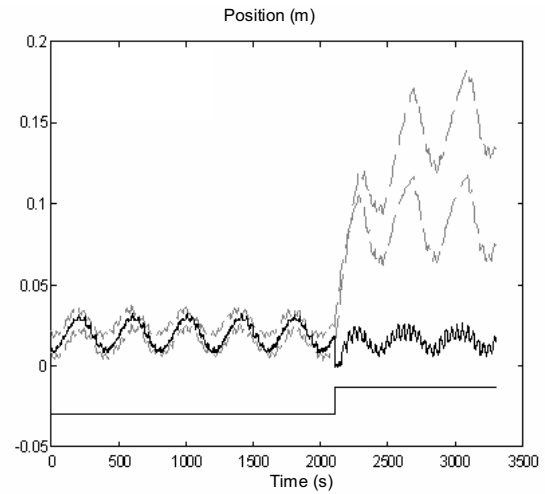

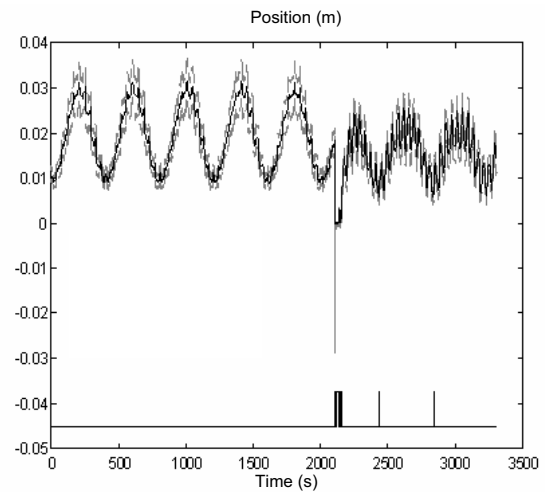Fig. 8. Fault detection of f_{10} using interval simulation.

Fig. 9. Fault detection of f_{10} using interval prediction.

sented in Fig. 11–13 confirm the same interpretations as in the case of f_{10}.

7.2.3. Discussion of results. From the application results presented so far, it can be observed that the simulation approach is most persistently sensitive to faults in the sense that when a fault appears its existence is constantly indicated, although it is very conservative (thick predic-
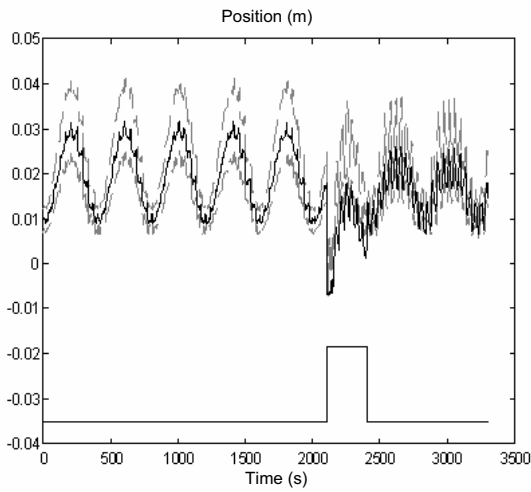
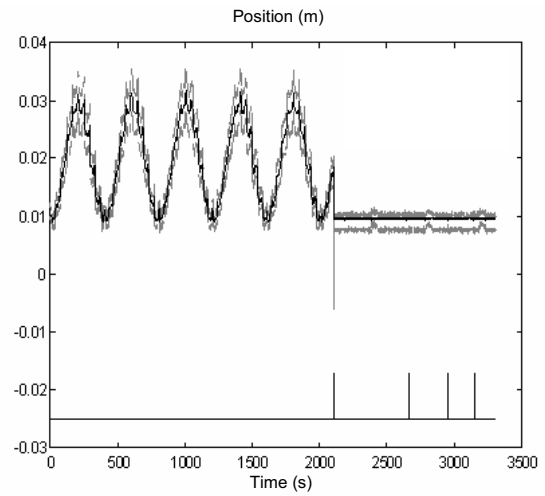Fig. 10. Fault detection of f_{10} using interval observation.

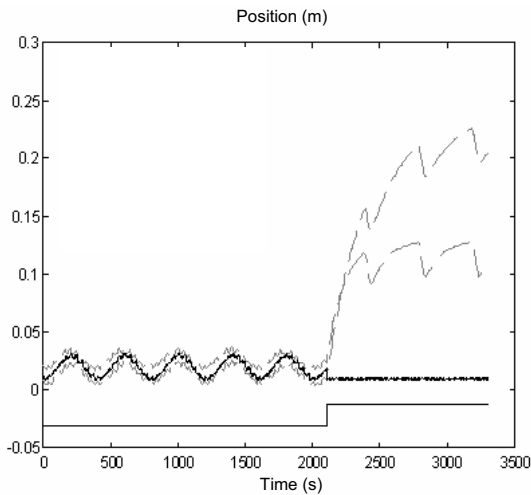Fig. 11. Fault detection of f_1 using interval simulation.

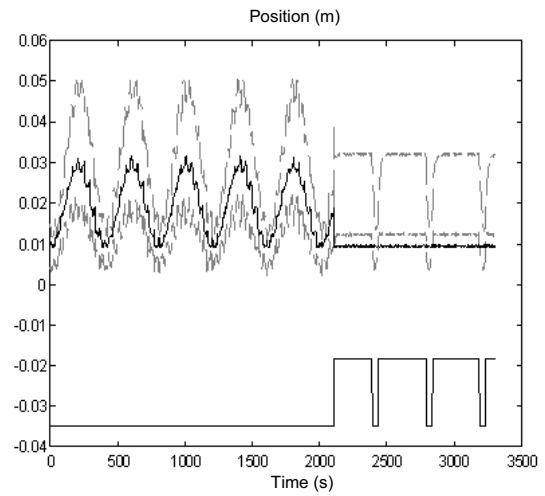Fig. 12. Fault detection of f_1 using interval prediction.

Fig. 13. Fault detection of f_1 using interval observation.

tion envelopes since no correction with measurements is introduced). On the other hand, the two other approaches are less conservative (tighter envelopes thanks to the correction with measurements) and very sensitive to faults when they appear, but also tend to follow the faulty system (*fault following effect*). However, when using an observer, designing properly the observer gain, the time to follow the fault can be increased. Regarding the effect of the noise on the different approaches, the prediction approach is very sensitive because it substitutes the output prediction by its measurement. The observation approach is less sensitive because of the correction of the output prediction is partial and controlled by the observer gain. Finally, the simulation approach is most insensitive to the noise effect of the three approaches because no correction of the output prediction is introduced. To deal with the noise, the test given by (3) is not usually sufficient. It

must be complemented with a more sophisticated test such as evaluating residual energy (Emami-Naeini *et al.*, 1988).

7.3. FTC application: Barcelona sewer network.

7.3.1. Introduction. Sewer networks are complex large-scale systems which, in turn, require highly sophisticated supervisory-control systems to ensure that high performance can be achieved and maintained under adverse conditions. Most cities around the world have sewage systems that combine sanitary and storm water flows within the same network. This is why these networks are known as *combined sewage systems* (CSSs). During rain storms, wastewater flows can easily overload these CSSs, thereby causing operators to dump the excess of water into the nearest receiver environment (rivers, streams or sea). This discharge to the environment, known as the *combined*

sewage overflow (CSO), contains biological and chemical contaminants creating a major environmental and public health hazard. A possible solution to the CSO problem is to use a highly sophisticated real-time control (RTC) scheme which ensures that high performance can be achieved and maintained under adverse meteorological conditions (Schütze *et al.*, 2004; Marinaki and Papageorgiou, 2005). Comprehensive reviews that include a discussion of some existing implementations are given by Schilling *et al.* (1996) and Schütze *et al.* (2004) and the cited references therein, while practical issues are discussed by Schütze *et al.* (2002), among others. The multivariable and large-scale nature of sewer networks has led to the use of some variants of model predictive control (MPC), as the control strategy widely use (Ocampo *et al.*, 2008).

The MPC control system need of operating in adverse meteorological conditions involves, with a high probability, sensor and actuator malfunctions (faults). This problem calls for the use of an on-line FD system able to detect and correct such faults (if possible) by activating fault tolerance mechanisms, such as soft sensors or embedded tolerance of the MPC controller, which allow avoiding stopping the control system every time a fault appears (Puig, 2009).

7.3.2. Fault tolerance evaluation. The case study to illustrate the MPC fault-tolerance evaluation approach presented in Section 6 corresponds to a piece of the Barcelona sewer network. The modelling methodology used to obtain a control oriented model of this network is based on the approach proposed by Gelormino and Ricker (1994) as well as Cembrano *et al.* (2004). In this methodology the sewer system is divided into connected subgroups of catchments and treated as interconnected *virtual tanks*. At any given time, the stored volume represents the amount of water inside the sewers. The volume is calculated through the mass balance of the stored volume, taking into account area rainfall and flow exchanges between the tanks. For each tank (catchment), the equation is

$$x_i(k+1) = x_i(k) + \varphi SP_i(k) \\ + \Delta t(q_i^{in}(k) - q_i^{out}(k)),$$

where φ is the ground absorption coefficient of the i-th catchment, S is the area of the i-th catchment, P is the precipitation intensity in Δt of the i-th catchment and Δt is the time interval between measurements. Here $q_i^{in}(k)$ and $q_i^{out}(k)$ are the sums of inflows and outflows, respectively. Using this modeling methodology, the model for the piece of the Barcelona sewer network considered is described by the following discrete-time state equations (Fig. 14):

$$\mathbf{v}_{k+1} = \mathbf{A}\mathbf{v}_k + \mathbf{B}\mathbf{q}_{u_k} + \mathbf{B}_p\mathbf{d}_k, \quad (43)$$

where

$$\mathbf{A} = \begin{pmatrix} 1 - \Delta t\beta_1 & 0 & 0 \\ 0 & 1 & 0 \\ \Delta t\beta_1 & 0 & 1 - \Delta t\beta_3 \end{pmatrix},$$

$$\mathbf{B} = \Delta t \begin{pmatrix} 1 & 0 & 0 \\ 0 & 1 & -1 \\ -1 & -1 & 1 \end{pmatrix},$$

$$\mathbf{B_P} = \Delta t \begin{pmatrix} 0 & \alpha_2 & 0 \\ 0 & 0 & 0 \\ 1 & 0 & \alpha_3 \end{pmatrix},$$

with sampling time $\Delta t = 300$ s and system parameters $\alpha_2 = 0.5715$, $\alpha_3 = 0.0783$, $\beta_1 = 5.8 \times 10^{-4}$ and $\beta_3 = 1.0 \times 10^{-3}$, which are estimated from real data. The system has three state variables v_i, corresponding to virtual/real tank volumes, and three input signals q_{u_i}, corresponding to the manipulated inflows by the command gates (Ocampo *et al.*, 2006). Vector d is related to the rain inflows (measured disturbances). The system constraints include:

- bounding constraints (refer to physical restrictions):

$$\begin{aligned} v_{2k} &\in [0, +\infty], & q_{u_1 k} &\in [0, 11], \\ v_{3k} &\in [0, 35000], & q_{u_2 k} &\in [0, 25], \quad (44) \\ v_{4k} &\in [0, +\infty], & q_{u_3 k} &\in [0, 7], \end{aligned}$$

- mass conservation constraints:

$$\begin{aligned} d_{1k} &= q_{u_1 k} + q_{14k}, \\ q_{v_1 k} &= q_{u_2 k} + q_{24k}, \quad (45) \\ q_{v_2 k} &\geq q_{u_3 k}, \end{aligned}$$

where $q_{v_i}(k) = \beta_i v_i(k)$ (Ocampo *et al.*, 2006). For the admissibility study, since it is done off-line, it is supposed that the vector d_k (rain) is known at each time instant k, which means a known perturbation. This means that the obtained results are used for the evaluation of the tolerant control system.

It is desired to evaluate the admissibility of different actuator fault configurations not only in reconfiguration but also in accommodation. Configuration admissibility is evaluated using Algorithm 6, which compares the control objectives degradation with respect to the nominal (without fault) configuration for a given rain episode. The selected rain episode corresponds to the one that occurred on September 14, 1999. This day severe flooding occurred as a consequence of a rain storm. The actuator faults are not simultaneous and they are present from the beginning of the scenario. Actuator faults are considered changes in the operating limits in the case of accommodation or as completely damaged in the case of reconfiguration.
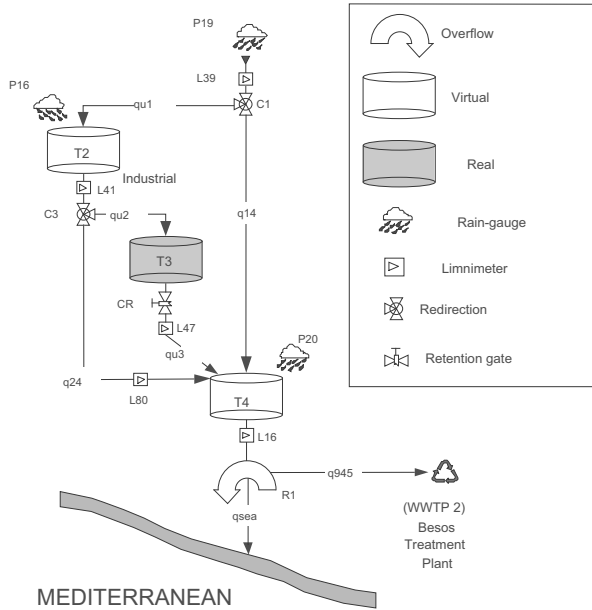
Fig. 14. Application case: three-tank catchment.

7.4. Control objective and admissibility criterion.
The control objective is defined as pollution (water volume that goes to the sea through collector q_{sea}). Thus, the control objective in terms of system variables can be written as follows:

$$J = V_{\text{sea}} = \Delta t \sum_{k=0}^{N} q_{\text{sea}}(k), \qquad (46)$$

where $q_{\text{sea}}(k) = \max(0, q_{v_3}(k) - q_3^{\max})$ is the water flow to sea.

The admissibility criterion is based on a direct comparison between the minimum volume in fault $V_{\text{sea}}^{\text{faulty}}$ and non-faulty configuration $V_{\text{sea}}^{\text{nom}}$. That is, setting α as the accepted level of degradation, if

$$V_{\text{sea}}^{\text{faulty}} > \alpha V_{\text{sea}}^{\text{nom}}, \qquad (47)$$

then the evaluated system configuration is not admissible. Otherwise, it is admissible. In the case study considered, the design condition α was set to 2 taking into account the heuristic knowledge of the system network operators.

7.5. Reconfiguration case. First, the case of actuators completely damaged due to a fault is considered. In particular, the case of gates completely closed is studied, that is, $q_{u_i} \in [0, 0]$ and $q_i \in [0, +\infty]$. The fault tolerant strategy that is used in this situation considers the reconfiguration of the control loop neglecting the faulty actuators. Admissibility evaluation results of each actuator fault configurations obtained applying Algorithm 6 are summarized

in Table 3. The second column shows the minimum value of water released to the sea at the end of the time horizon considered. Figure 15 shows the minimum feasible volume released to the sea (pollution) for each actuator fault configuration compared against the admissibility threshold (47) when reconfiguration is used.

Table 3. Admissibility of fault configurations for pollution: reconfiguration.

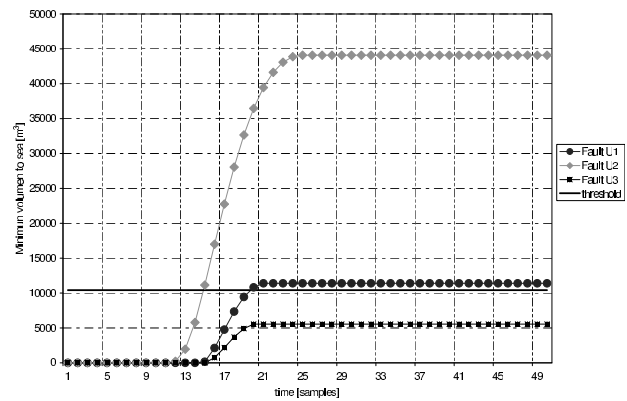| Fault location	Min. volume [m^3]	Admissibility status
No fault	5209	—
Fault in q_{u_1}	11395	Not admissible
Fault in q_{u_2}	44089	Not admissible
Fault in q_{u_3}	5209	Admissible

Fig. 15. Minimum volume to the sea in different fault scenarios in reconfiguration.

7.6. Accommodation case. Now, faults that cause a reduction in the actuator operating range (for example from 0–100% to 0–50%) are considered. The fault tolerant strategy that is used in this case is based on accommodating the controller by changing the actuator operating ranges according to the fault. Application of Algorithm 6 to two accommodation ranges for each actuator fault configuration are considered. The results of admissibility evaluation are summarized in Table 4. This table does not consider the case of a fault in q_{u_3} due to system insensitivity to this actuator fault, as shown in Table 3. Figure 16 shows the minimum feasible volume released to the sea (pollution) for each actuator fault configuration compared against the admissibility threshold (47) when accommodation is used.

8. Conclusions

This paper has reviewed the use of set-membership methods in robust FD and FTC. Alternatively to statistical methods, set-membership methods use a deterministic

Table 4. Admissibility of fault configurations: accommodation

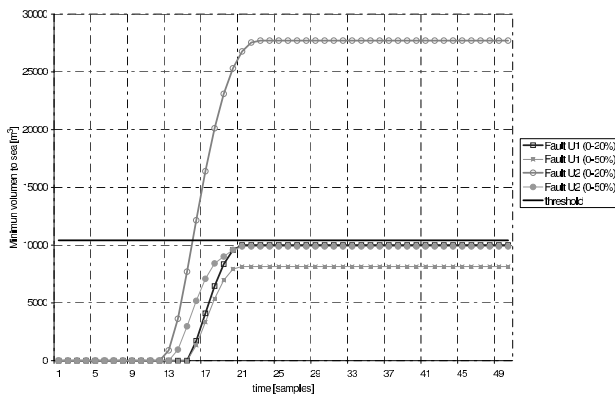| Fault location	Operation range	Min. volume [m³]	Admissibility status
No fault	—	5209	—
Fault in q_{u_1}	0-20%	10005	Admissible
Fault in q_{u_1}	0-50%	8149	Admissible
Fault in q_{u_2}	0-20%	27705	Not Admissible
Fault in q_{u_2}	0-50%	9887	Admissible

Fig. 16. Minimum volume to the sea in different fault scenarios in accomodation

unknown-but-bounded description of noise and parametric uncertainty (interval models). Using approximating sets to enclose the exact set of possible behaviours (in the parameter or the state space), these methods allow checking the consistency between the observed and predicted behaviours. When an inconsistency is detected the fault can be indicated, otherwise nothing can be stated. The same principle has been used to estimate interval models for fault detection and to develop methods for fault tolerance evaluation. Finally, a real application of these methods has been used to exemplify the successful use of the proposed set-membership methods in FD/FTC.

Acknowledgment

References

Ackermann, J. (2002). *Robust Control: The Parameter Space Approach*, Springer, London.

Adrot, O. and Flaus, J.M. (2008). Fault detection based on uncertain models with bounded parameters and bounded parameter variations, *Proceedings of the 17th IFAC World Congress, Seoul, Korea*, pp. 7338–7343.

Alamo, T., Bravo, J. and Camacho, E. (2005). Guaranteed state estimation by zonotopes, *Automatica* **41**(6): 1035–1043.

Armengol, J., Travé-Massuyès, L., Vehí, J. and de la Rosa, J.L. (2000). A survey on interval model simulators and their properties related to fault detection, *Annual Reviews in Control* **24**: 31–39.

Armengol, J., Vehí, J., Sainz, M., Herrero, P. and Gelso, E. (2008). Squaltrack: A tool for robust fault detection, *IEEE Transactions on Systems, Man, and Cybernetics: Part B* **39**(2): 475–488.

Bartyś, M. and de las Heras, S. (2003). Actuator simulation of the damadics benchmark actuator system, *Proceedings of IFAC SAFEPROCESS'03, Washington, DC, USA*.

Bartys, M., Patton, R., de las Heras, S., Syfert, M. and Quevedo, J. (2006). Introduction to the Damadics actuator FDI benchmark study, *Control Engineering Practice* **14**(6): 577–596.

Bhattacharyya, S., Chapellat, H. and Keel, L. (1995). *Robust Control: The Parametric Approach*, Prentice Hall PTR, Upper Saddle River, NJ.

Bravo, J., Alamo, T. and Camacho, E. (2006). Bounded error identification of systems with time-varying parameters, *IEEE Transactions on Automatic Control* **51**(7): 1144–1150.

Calafiore, G. (2001). A set-valued non-linear filter for robust localization, *Proceedings of the European Control Conference (ECC'01), Porto, Portugal*.

Calafiore, G., Campi, M.C. and Ghaoui, L.E. (2002). Identification of reliable predictor models for unknown systems: A data-consistency approach based on learning theory, *Proceedings of the 15th IFAC World Congress, Barcelona, Spain*.

Campi, M. and Calafiore, S.G. (2009). Interval predictor models: Identification and reliability, *Automatica* **45**(8): 382–391.

Cembrano, G., Quevedo, J., Salamero, M., Puig, V., Figueras, J. and Martí, J. (2004). Optimal control of urban drainage systems: A case study, *Control Engineering Practice* **12**(1): 1–9.

Chen, J. and Patton, R. (1999). *Robust Model-Based Fault Diagnosis for Dynamic Systems*, Kluwer Academic Publishers, Boston, MA.

Chilali, M. and Gahinet, P. (1996). H_∞ design with pole placement constraints: An LMI approach, *IEEE Transactions on Automatic Control* **41**(3): 358–367.

Chisci, L., Garulli, A. and Zappa, G. (1996). Recursive state bounding by parallelotopes, *Automatica* **32**(3): 1049–1055.

Emami-Naeini, A., Akhter, M. and Rock, S. (1988). Effect of model uncertainty on failure detection: The threshold selector, *IEEE Transactions on Automatic Control* **AC-33**(12): 1106–1115.

Escobet, T., Travé-Massuyès, L., Tornil, S. and Quevedo, J. (2001). Fault detection of a gas turbine fuel actuator based on qualitative causal models, *Proceedings of the European Control Conference (ECC'01), Porto, Portugal*.

Fagarasan, I., Ploix, S. and Gentil, S. (2004). Causal fault detection and isolation based on a set-membership approach, *Automatica* **40**(12): 2099–2110.

Gelormino, M. and Ricker, N. (1994). Model-predictive control of a combined sewer system, *International Journal of Control* **59**(3): 793–816.

Gertler, J. (1998). *Fault Detection and Diagnosis in Engineering Systems*, Marcel Dekker, New York, NY.

Guerra, P., Ocampo-Martinez, C. and Puig, V. (2007). Actuator fault tolerance evaluation of linear constrained robust model predictive control, *Proceedings of the IEEE European Control Conference (ECC'07), Kos, Greece*.

Guerra, P., Puig, V. and Ingimundarson, A. (2007). Robust fault detection using a consistency-based state estimation, *Proceedings of the IEEE European Control Conference (ECC'07), Kos, Greece*.

Guerra, P., Puig, V. and Witczak, M. (2008). Robust fault detection with unknown-input interval observers using zonotopes, *Proceedings of the 17th IFAC World Congress, Seoul, Korea*, pp. 5557–5562.

Hamelin, F. and Sauter, D. (2000). Robust fault detection in uncertain dynamic systems, *Automatica* **36**(11): 1747–1754.

Hansen, E. (1992). *Global Optimization Using Interval Analysis*, Marcel Dekker, New York, NY.

Horak, D. (1988). Failure detection in dynamic systems with modelling errors, *AIAA Journal of Guidance, Control and Dynamics* **11**(6): 508–516.

Ingimundarson, A., Bravo, J., Puig, V., Alamo, T. and Guerra, P. (2008). Robust fault detection using zonotope-based set-membership consistency test, *Journal of Adaptive Control and Signal Processing* **23**(4): 311–330.

Isermann, R. (2006). *Fault Diagnosis Systems: An Introduction from Fault Detection to Fault Tolerance*, Springer, New York, NY.

Kieffer, M., Jaulin, L. and Walter, E. (2002). Guaranteed recursive non-linear state bounding using interval analysis, *International Journal of Adaptive Control and Signal Processing* **16**(3): 193–218.

Kolev, L. (1993). *Interval Methods for Circuit Analysis*, World Scientific, Singapore.

Kuipers, B. (1994). *Qualitative Reasoning—Modelling and Simulation with Incomplete Knowledge*, MIT Press, Cambridge, MA.

Lydoire, F. and Poignet, P. (2005). Non-linear predictive control using constraints satisfaction, *in* C. Jermann, A. Neumaier and D. Sam (Eds.), *Global Optimization and Constraints Satisfaction*, Lecture Notes in Computer Science, Vol. 3478, Springer-Verlag, pp. 142–153.

Maksarov, D. and Norton, J. (1996). State bounding with ellipsoidal set description of the uncertainty, *International Journal of Control* **65**(5): 847 – 866.

Marinaki, M. and Papageorgiou, M. (2005). *Optimal Real-time Control of Sewer Networks*, Springer, London.

Milanese, M., Norton, J., Piet-Lahanier, H. and Walter, E. (1996). *Bounding Approaches to System Identification*, Plenum Press, New York, NY.

Montgomery, H. (1989). Computing the volume of a zonotope, *American Mathematical Monthly* **96**: 431.

Ocampo, C., Ingimundarson, A., Puig, V. and Quevedo, J. (2008). Objective prioritization using lexicographic minimizers for MPC of sewer networks, *IEEE Transactions on Control Systems Technology* **16**(1): 113–121.

Ocampo, C., Puig, V. and Quevedo, J. (2006). Actuator fault tolerance evaluation of constrained nonlinear MPC using constraints satisfaction, *Proceedings of IFAC SAFEPROCESS'06, Beijing, China*.

Ocampo, C., Tornil, S. and Puig, V. (2006). Robust fault detection using interval constraints satisfaction and set computations, *Proceedings of IFAC SAFEPROCESS'06, Beijing, China*.

Planchon, P. and Lunze, J. (2006). Robust diagnosis using state estimation, *Proceedings of IFAC SAFEPROCESS'06, Beijing, China*.

Ploix, S. and Adrot, O. (2006). Parity relations for linear uncertain dynamic systems, *Automatica* **42**(6): 1553–1562.

Ploix, S., Adrot, O. and Ragot, J. (1999). Parameter uncertainty computation in static linear models, *Proccedings of the 38th IEEE Conference on Decision and Control, Phoenix, AZ, USA*.

Puig, V. (2009). Fault detection and isolation in sewer networks, *Proceedings of IFAC SAFEPROCESS'09, Barcelona, Spain*.

Puig, V., Quevedo, J., Escobet, T., Nejjari, F. and de las Heras, S. (2008). Passive robust fault detection of dynamic processes using interval models, *IEEE Transactions on Control Systems Technology* **16**(5): 1083–1089.

Puig, V., Saludes, J. and Quevedo, J. (2003). Worst-case simulation of discrete linear time-invariant interval dynamic systems, *Reliable Computing* **9**(4): 251–290.

Puig, V., Stancu, A., Escobet, T., Nejjari, F., Quevedo, J. and Patton, R. (2006). Passive robust fault detection using interval observers: Application to the DAMADICS benchmark problem, *Control Engineering Practice* **14**(6): 621–633.

Rambeaux, F., H. F. S. D. (2000). Optimal thresholding for robust fault detection of uncertain systems, *International Journal of Robust and Nonlinear Control* **10**(14): 1155–1173.

Rinner, B. and Weiss, U. (2004). Online monitoring by dynamically refining imprecise models, *IEEE Transactions on Systems, Man, and Cybernetics: Part B* **34**(4): 1811–1822.

Rugh, W. and Shamma, J. (2000). A survey of research on gain-scheduling, *Automatica* **36**(10): 1401–1425.

Sainz, M., Armengol, J. and Vehí, J. (2002). Fault detection and isolation of the three-tank system using the modal interval analysis, *Journal of Process Control* **12**(2): 325–338.

Schilling, W., Anderson, B., Nyberg, U., Aspegren, H., Rauch, W. and Harremöes, P. (1996). Real-time control of wasterwater systems, *Journal of Hydraulic Resources* **34**(6): 785–797.

Schütze, M., Campisano, A., Colas, H., Schilling W. and Vanrolleghem, P. (2004). Real time control of urban wastewater systems: Where do we stand today?, *Journal of Hydrology* **299**: 335–348.

Schütze, M. and Beck, B. (2002). *Modelling, Simulation and Control of Urban Wastewater Systems*, Springer, London.

Shamma, J. (1997). Approximate set-value observer for nonlinear systems, *IEEE Transactions on Automatic Control* **42**(5): 648–658.

Staroswiecki, M. (2003). Actuator faults and the linear quadratic control problem, *Proceedings of the IEEE Conference on Decision and Control, Maui, HI, USA*, pp. 959–965.

Tornil, S., Escobet, T. and Travé-Massuyès, L. (2003). Robust fault detection using interval models, *Proceedings of the European Control Conference (ECC'03), Cambridge, UK*.

Travé-Massuyes, L., Escobet, T., Pons, R. and Tornil, S. (2001). The CA EN diagnosis system and its automatic modelling method, *Computación y Sistemas* **5**(2): 648–658, (in Spanish).

Vicenç Puig received the Ph.D. degree in control engineering in 1999 and the telecommunications engineering degree in 1993, both from Universitat Politècnica de Catalunya (UPC), Barcelona, Spain. He is currently an associate professor of automatic control and the leader of the Advanced Control Systems (SAC) research group at Universitat Politècnica de Catalunya. His main research interests are fault detection and isolation of fault-tolerant control of dynamic systems. He has been involved in several European projects and networks and has published several papers in scientific journals and international conference proceedings.